

# Mathematical Modelling of Digit Specification by a Sonic Hedgehog Gradient

Thomas E. Woolley,<sup>1,2</sup> Ruth E. Baker,<sup>1</sup> Cheryll Tickle,<sup>3</sup> Philip K. Maini,<sup>1</sup> and Matthew Towers<sup>4\*</sup>

**Background:** The three chick wing digits represent a classical example of a pattern specified by a morphogen gradient. Here we have investigated whether a mathematical model of a Shh gradient can describe the specification of the identities of the three chick wing digits and if it can be applied to limbs with more digits. **Results:** We have produced a mathematical model for specification of chick wing digit identities by a Shh gradient that can be extended to the four digits of the chick leg with Shh-producing cells forming a digit. This model cannot be extended to specify the five digits of the mouse limb. **Conclusions:** Our data suggest that the parameters of a classical-type morphogen gradient are sufficient to specify the identities of three different digits. However, to specify more digit identities, this core mechanism has to be coupled to alternative processes, one being that in the chick leg and mouse limb, Shh-producing cells give rise to digits; another that in the mouse limb, the cellular response to the Shh gradient adapts over time so that digit specification does not depend simply on Shh concentration. *Developmental Dynamics* 243:290–298, 2014. © 2013 Wiley Periodicals, Inc.

**Key words:** limb; Shh; gradient; morphogen; mathematical modelling; chick wing; diffusion; digits; growth

## Key findings:

- A mathematical model based on localised production, diffusion and decay of Shh can specify the identities of the different digits in chick wing and leg.
- The model predicts that the amount of Shh produced by the polarizing region increases over time.
- Growth is an integral part of the model.
- The mathematical model cannot be simply extended to specify the identities of the five digits in the mouse limb.
- Mechanisms in addition to a simple morphogen gradient are required to specify the identities of five digits.

Submitted 25 March 2013; Last Decision 17 September 2013; Accepted 18 September 2013

## INTRODUCTION

One of the best-studied examples of pattern formation in vertebrate embryos is development of the three morphologically distinct digits in the chick wing (Towers and Tickle, 2009). Classical experiments led to the dis-

covery of the polarizing region, or zone of polarizing activity (ZPA), a signalling region at the posterior margin of the chick wing bud (Saunders and Gasseling, 1968). When an additional polarizing region is grafted to the anterior margin of a host wing bud, striking mirror image duplica-

tions of the normal chick wing pattern of three digits (1, 2 and 3) arise, giving patterns such as 3,2,1,1,2,3 (Saunders and Gasseling, 1968; Tickle et al., 1975) [note revised digit numbering: bird digits arise in embryonic positions 1, 2, and 3 (Towers et al., 2011) and not 2, 3, and 4

<sup>1</sup>Wolfson Centre for Mathematical Biology, Mathematical Institute, University of Oxford, Radcliffe Observatory Quarter, Oxford, United Kingdom

<sup>2</sup>Oxford Centre for Collaborative Applied Mathematics, Mathematical Institute, University of Oxford, Oxford, United Kingdom

<sup>3</sup>Department of Biology and Biochemistry, University of Bath, Bath, United Kingdom

<sup>4</sup>MRC centre of Developmental and Biomedical Genetics, University of Sheffield, Sheffield, United Kingdom

Grant sponsor: King Abdullah, University of Science and Technology (KAUST); Grant number: KUK-C1-013-04.

The authors declare no competing financial interests

\*Correspondence to: Matthew Towers, MRC Centre of Developmental and Biomedical Genetics, University of Sheffield, Western Bank, Sheffield, S10 2TN, UK. E-mail: m.towers@sheffield.ac.uk

DOI: 10.1002/dvdy.24068

Published online 2 October 2013 in Wiley Online Library (wileyonlinelibrary.com).

(Tamura et al., 2011)]. To explain these findings, it was proposed that the polarizing region produces a diffusible morphogen that sets up a gradient across the wing bud; cells at different positions would be exposed to different morphogen concentrations, thus providing them with the positional value required to form the appropriate digit (Wolpert, 1969; Tickle et al., 1975). This is widely known as the French Flag Model (Wolpert, 1969). There is experimental evidence that polarizing region signalling specifies digits over time (Smith, 1980) in a concentration-dependent manner (Smith et al., 1978; Tickle, 1981). Polarizing region signalling was also shown to act over a long-range (Honig, 1981) consistent with the morphogen gradient model (Wolpert, 1969). Furthermore, although not a key component of the morphogen model, polarizing region grafts were also shown to promote S-phase entry (Cooke and Summerbell, 1980) leading to widening of the bud.

It is now established that the *Sonic hedgehog* (*Shh*) gene is expressed by polarizing region cells of the chick wing bud (Riddle et al., 1993) and that the Sonic hedgehog protein displays all the characteristics of the polarizing region morphogen (Yang et al., 1997), including acting as a proliferative signal that determines the size of the digit-forming field and digit number (Towers et al., 2008). Dye-labelled fate maps show the positions that the digits arise from in the posterior third of the wing bud (Vargesson et al., 1997; Towers et al., 2008). There is also evidence that the Shh protein concentration is graded across the bud (Zeng et al., 2001). Recent fate maps based on grafts of GFP-expressing tissue demonstrate that the polarizing region does not contribute to the skeletal pattern, thus confirming that all three chick wing digits are specified by long-range signalling (Towers et al., 2011). It has also been shown that cells first acquire anterior positional values before being promoted to increasingly posterior positional values every 4 hr, hence 12 hr in total is required to specify the most-posterior digit identity (Tickle, 1995; Towers et al., 2011).

Several mathematical models have focussed on reproducing the periodic

pre-pattern of digit condensations (Wilby and Ede, 1975; Newman and Frisch, 1979; Hentschel et al., 2004; Izaguirre et al., 2004; Newman et al., 2008), often using Turing and related mechanisms, with only a few attempts made to understand how this periodic pre-pattern integrates with the earlier external gradient (Benson et al., 1993; Glimm et al., 2012a,b; Crampin et al., 1999). Wolpert and Hornbruch (1981) produced a mathematical model based on a morphogen gradient, using theoretical parameters, to reproduce the final state of the chick wing digit pattern. In this model, the gradient specified the number of digits as well as their identities. The purpose of this model was to demonstrate how long-range signalling rather than local cell-cell interactions (French et al., 1976) could best explain the digit patterns obtained when polarizing regions were grafted at varying distances apart. However, despite this model providing useful insights, the experimental parameters needed for making a realistic morphogen gradient model were only obtained shortly afterwards, including the concentration-dependency and the long-range nature of the then unknown signal (Tickle, 1981; Honig, 1981). Since 1981, it has been discovered that Shh acts as the morphogen and the parameters of morphogen function based on Shh function have been determined allowing models to be built that have more biological relevance (Experimental procedures). One of the first of these models was from Dillon et al. who modelled the dynamic changes in *Ptch1* expression induced by Shh-soaked beads and polarizing region grafts made to anterior margins of the chick wing and concluded that Shh can act long-range (Dillon et al., 2003; also see Drossopoulou et al., 2000). However, except for Hentschel et al. (2004), no simulation has considered growth of the wing bud, although it is clear that this is essential for specifying the correct number of digits (Towers et al., 2008). Further, no model has considered the consecutive anterior-to-posterior promotion sequence of digit specification (Tickle, 1995). Knowing in quantitative detail how Shh specifies the three digits of the chick wing

(Experimental procedures) has allowed us to carry out mathematical simulations to see if this promotion sequence is consistent with a gradient-based mechanism comprising localised production, diffusion, and decay of Shh. We then explored whether the same model is applicable to the chick leg with four digits and finally the mouse limb with five digits.

## RESULTS

### Mathematical Modelling of Digit Specification in the Chick Wing

Several parameters are needed to model chick wing digit specification by an Shh gradient based on production, diffusion, and decay. These are the size of the digit-forming field and the positions within the field from which the digits arise; the growth rate of the digit-forming field over the time period of digit specification; the concentration thresholds at which Shh specifies the different digits; and the degradation and diffusion rates of Shh (Experimental procedures). Unlike the model of Wolpert and Hornbruch (1981), in which the digit positions were specified by the gradient itself, in our model digit positions are specified as being equally-spaced within the digit-forming region, with a defined minimum width per digit (see Experimental procedures), thus, implementing a simple periodic mechanism that is independent of the Shh gradient (which could be representing a Turing-type mechanism) (Wilby and Ede, 1975; Newman and Frisch, 1979; Hentschel et al., 2004; Izaguirre et al., 2004; Newman et al., 2008).

At the outset, our model consists of a one-dimensional representation of the early Hamilton Hamburger stage 18/19 chick wing bud, which is approximately 600  $\mu\text{m}$  across (in width) (Fig. 1). The wing bud is divided into three regions; the posterior 100  $\mu\text{m}$  composed of polarizing region cells, which produce Shh that diffuses across the adjacent 300  $\mu\text{m}$  digit-forming field and the anterior 200  $\mu\text{m}$ . Although cells in the anterior region do not contribute to digit development, we include this domain in our model so that we can apply a

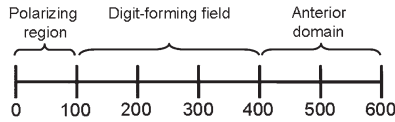


**Fig. 1.** One-dimensional static model of the stage-18/19 chick wing bud. Shh is produced in the polarizing region at the posterior margin of the bud and diffuses into the adjacent digit-forming field that gives rise to three digits. The anterior part of the bud does not give rise to digits. Measurements in microns.

natural (zero flux) boundary condition at the anterior edge of the wing bud. We have not considered receptor molecules that could sequester Shh at the cell surface and limit diffusion such as *Ptch1*, *Boc1*, *Cdo1*, and *Gas1*. During the 12-hr period of digit specification, *Ptch1* is expressed at high levels in the polarizing region and at weaker levels adjacently (Marigo et al., 1996), suggesting it could fulfil a role in trapping Shh in the polarizing region and not interfering with the pool of freely diffusible Shh that we have modelled. *Gas1*, *Cdo1*, and *Boc1* are expressed anteriorly (Allen et al., 2011) so could limit the diffusion of Shh out of the digit-forming field. Thus it is likely that cell surface regulators of Shh signalling modify posterior and anterior boundary conditions and do not greatly modulate free diffusion of Shh.

We tested whether we could produce a model of graded Shh signalling sufficient to specify the identities of the three chick wing digits. At the outset, the Shh concentration in the polarizing region is considered to be zero, with growth of the polarizing region allowing total production rate

of Shh to increase with time. We solve the diffusion equation with linear decay on a uniformly linearly growing domain of initial length 600  $\mu\text{m}$ .

Nonlinear forms of decay have also been considered (data not shown). It was found that altering the decay parameter to account for the higher nonlinearities, the difference between linear, quadratic, and cubic decay is too small to cause significant differences in the final digit profiles. Nonlinearities cause the decay of Shh from the polarizing region to be sharper, leading to a shallower gradient in the rest of the digit-forming field. This shallower gradient means that the concentration range is not great enough to cross all the desired thresholds for specifying each digit at the correct spatial positions. Under our current assumptions of using a diffusive signal, this and previous modelling work (Dillon et al., 2003), indicate that linear degradation is a good approximation to the underlying dynamics.

Since Shh cannot pass through the physical boundaries at either margin of the wing bud (zero flux), we derive the following set of equations,

$$\frac{\partial u}{\partial t} + \frac{\partial(vu)}{\partial x} = D \frac{\partial^2 u}{\partial x^2} + s(x) - \gamma u, \quad x \in [0, 600(1 + rt)], \quad (1)$$

$$\frac{\partial u}{\partial x}(0, t) = 0, \quad \frac{\partial u}{\partial x}(600(1 + rt), t) = 0, \quad u(x, 0) = 0, \quad (2)$$

where the concentration of Shh,  $u$ , diffusivity,  $D$ , and degradation rate,  $\gamma$ ,

have units  $\text{nM}/\mu\text{m}$ ,  $\mu\text{m}^2/\text{s}$  and  $1/\text{s}$ , respectively.  $v = rx/(1 + rt)$  is the velocity field of the flow generated by the uniform linear domain growth (see Crampin et al., 1999) for details). The spatially inhomogeneous source term  $s(x)$  has the form

$$s(x) = \begin{cases} \alpha t & \text{for } x < 100(1 + rt), \\ 0 & \text{for } x > 100(1 + rt), \end{cases} \quad (3)$$

which constrains production of Shh to the polarizing region. To solve these equations we mapped the growing wing domain back to an equivalent stationary domain (Crampin et al., 1999). This set of equations leads to the Shh concentration doubling over the correct temporal scale so that the digits are specified by 12 hr with promotion occurring at 4-hr intervals (Fig. 2, Supp. Movie S1, which is available online).

### Importance of Growth in Digit Specification in the Chick Wing

We asked if our simulation could recapitulate experimental results of manipulating expansion of the wing bud by applying cell proliferation inhibitors during the digit specification phase to transiently inhibit growth (Towers et al., 2008). When expansion of the digit-forming field was halved so that it expanded from only 300 to 375  $\mu\text{m}$  (instead of from 300 to 450  $\mu\text{m}$ ), three digits still formed. This means that the minimum size for a digit domain is 125  $\mu\text{m}$ . This estimate is consistent with other data obtained when growth was inhibited still further, with two digits (digits 2 and 3) forming when bud width remained constant and only one digit (digit 3) when the bud width was reduced by 100  $\mu\text{m}$  (Towers et al., 2008). The digits that formed under these conditions were posterior digits because promotion of digit identity by Shh occurred as normal. When we simulated these growth conditions, the number of digits was reduced. Furthermore, anterior digit identities were indeed lost under the most restrictive conditions, although to make the gradient breach the level required to specify digit 3 at the correct time, we had to increase the source term slightly (the Shh production rate) to compensate for the

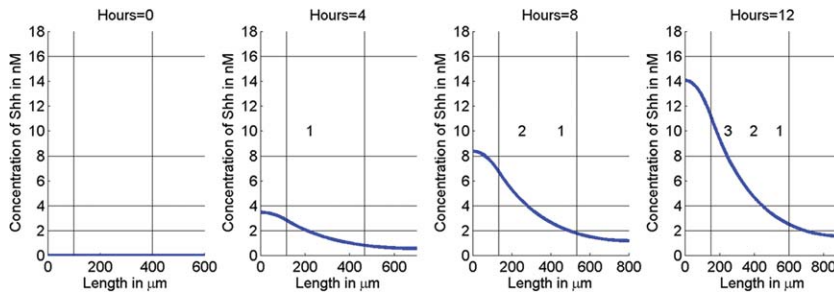


**Fig. 2.** (Supp. Movie S1). Simulation of chick wing digit specification by an Shh gradient. The blue line is the solution of equation (1) with boundary conditions given by equation (2) and source given by equation (3) on a uniformly linearly growing domain. Parameters are  $D = 24 \mu\text{m}^2/\text{s}$ ,  $\gamma = 1/60^2 1/\text{s}$ ,  $\alpha = 0.014/57600^2/\text{s}$  and  $r = 0.5/43200/\text{s}$ . The two vertical black lines delineate the domain into the three sections, as described in Figure 1. The vertical red lines delineate the digit domains. The horizontal black lines illustrate the thresholds required for each digit identity. These lines are consistently shown on all plots. Digits are specified over the correct time period with promotion occurring every 4 hr.



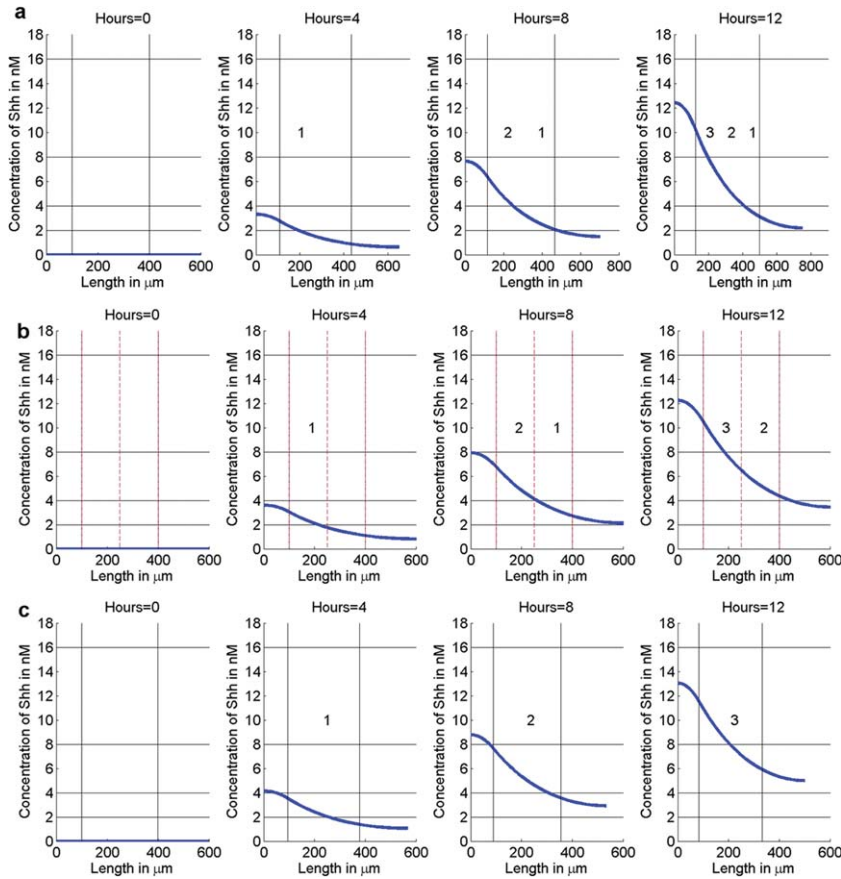


**Fig. 3.** (Supp. Movies S2–4). Simulations of chick wing digit specification following growth arrest. Solution of equation (1) with boundary conditions given by equation (2) and source given by equation (3) on a reduced growth domain (a), stationary domain (b), and a uniformly linearly shrinking domain (c). Parameters are  $D = 24 \mu\text{m}^2/\text{s}$  and  $\gamma = 1/60^2/\text{s}$  in all simulations and (a)  $\alpha = 0.019/57600^2/\text{s}$  and  $r = 0.25/43200/\text{s}$ , (b)  $\alpha = 0.016/57600^2/\text{s}$  and  $r = 0/\text{s}$  and (c)  $\alpha = 0.019/57600^2/\text{s}$  and  $r = -1/(6 \times 43200)/\text{s}$ . a, Movie 2: Normal pattern results when expansion of the digit-field is halved. b, Movie 3: Two posterior digits form when growth is arrested in chick wing buds. c, Movie 4: Only the most-posterior digit forms when the size of the digit-forming field diminishes in chick wing buds.

reduction in growth of the polarizing region itself (Fig. 3a–c, Supp. Movies S2–4). Interestingly, in agreement with this requirement, we had noticed that at the start of the digit specification phase following transient growth inhibition there is indeed a dramatic increase in *Shh* transcripts (Towers et al., 2008). These results show that if bud width is reduced, the resulting gradient gives a good approximation of the temporal sequence of digit promotion over the correct time period.

### Mathematical Modelling of Digit Specification in the Chick Leg

Having validated a basic mathematical model of the temporal pattern of

digit specification for the chick wing, we asked whether a similar model could generate the four different digits of the chick leg. The first three anterior digits in both chick wing (1, 2, and 3) and chick leg (I, II, and III) are homologous and are specified over 12 hr so we used the same model parameters (Towers et al., 2011). Digit IV in the chick leg arises from the polarizing region and progenitor cells are sequentially promoted every 4 hr through anterior digit identities I, II, III, and then finally IV after 16 hr (Towers et al., 2011). We have assumed that this graded specification of successive digit identities in leg-polarizing region cells involves a doubling in *Shh* concentration, i.e., digit IV in the leg would require 16 nM, double the *Shh* concentration

that specifies digit III. This assumption is based on the following observations. When *Shh* signalling is inhibited in the chick leg using cyclopamine, digit IV is most frequently lost than any of the other digits, suggesting that a higher level of *Shh* specifies digit IV than the other three digits (Scherz et al., 2007; Towers et al., 2011) and wing-polarizing region grafts made to the anterior margin of the leg bud specify a leg digit III adjacently (Summerbell and Tickle, 1977, Towers et al., 2011). In addition, when a normal leg-polarizing region is grafted to the posterior margin of an *Oligozeugodactyly* mutant wing bud, which lacks *Shh* function, three wing digits arise in host tissue adjacent to a leg digit emanating from the donor graft (Ros et al., 2003). Taken together, these findings suggest that the local concentration of *Shh* released by wing- and leg-polarizing regions is comparable and that a higher level of *Shh* specifies the most-posterior digit of the leg than the most-posterior digit of the wing.

We found that simulating the chick wing model for a further 4 hr resulted in an accurate representation of chick leg digit identity specification (Towers et al., 2011). Moreover, the gradient breached the thresholds required to give the digit pattern I, I at 4 hr, I, II, II at 8 hr, I, II, III, III at 12 hr, and I, II, III, IV at 16 hr (Fig. 4, Supp. Movie S5; taking into account that one digit arises from the polarizing region). This is precisely the sequence of digit patterns seen when *Shh* signalling is inhibited experimentally at different time points (Towers et al., 2011).

### Mathematical Modelling of Digit Specification in the Mouse Limb

In the mouse limb, two digits, 4 and 5, arise completely from the polarizing region. It is unclear whether digit 1 requires *Shh* function as it forms in hindlimbs but not forelimbs lacking *Shh* function (Chiang et al., 1996). In addition, the amount of *Shh* required to specify the equivalent digit 1 in chick wing, the amount produced by as few as ten cells (Tickle, 1981), must be extremely low, making it

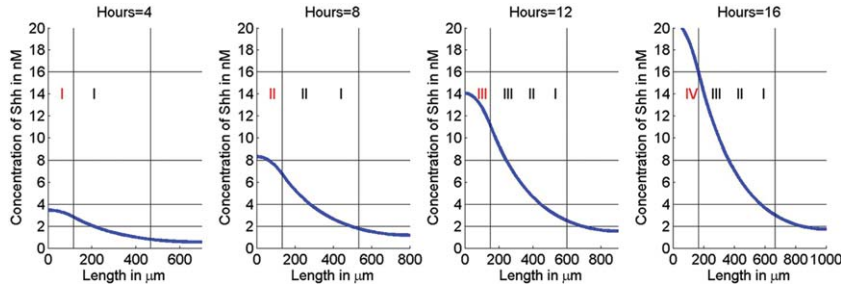


**Fig. 4.** (Supp. Movie S5). Simulation of chick leg digit specification by an Shh gradient. Solution of equation (1) with boundary conditions given by equation (2) and source given by equation (3), on a uniformly linearly growing domain. Parameters are  $D = 24 \mu\text{m}^2/\text{s}$ ,  $\gamma = 1/60^2/\text{s}$ ,  $\alpha = 0.014/57600^2/\text{s}$  and  $r = 0.5/(43200)/\text{s}$ . Digits arising from the polarizing region are coloured red. Digits are specified over the correct time period with promotion occurring every 4 hr.

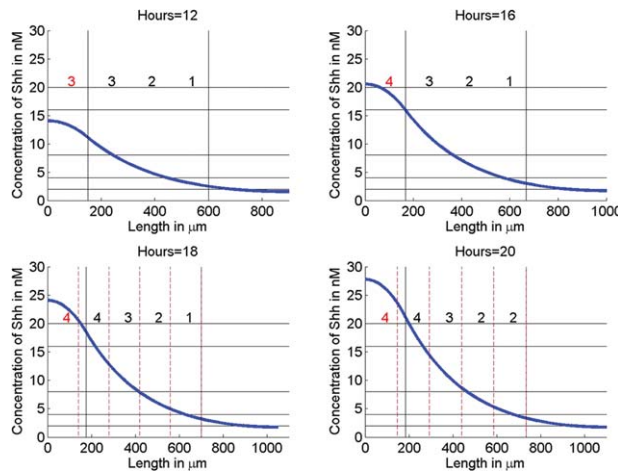


**Fig. 5.** (Supp. Movie S6). Simulation of mouse digit patterning by an Shh gradient. Solution of equation (1) with boundary conditions given by equation (2) and source given by equation (3), on a uniformly linearly growing domain. Parameters are  $D = 24 \mu\text{m}^2/\text{s}$ ,  $\gamma = 1/60^2/\text{s}$ ,  $\alpha = 0.014/57600^2/\text{s}$  and  $r = 0.5/(43200)/\text{s}$ . Plots for 4–16 hr are the same as in Figure 4. A pattern with five digits 2,2,3,4,4 is produced instead of the normal pattern 1,2,3,4,5. Only one digit arises from the polarizing region (shown in red) whereas normally two do so.

difficult to observe in progenitor cells of this digit as determined by a *Gli1* reporter transgene, which might not give an accurate read-out of Shh signalling (Ahn and Joyner, 2004). To examine whether specification of the identities of the five mouse limb digits by an Shh gradient could be a simple extension of the chick leg model, we simulated the chick leg model for another 4 hr (20 hr in total) and set the threshold concentration of Shh to specify digit 5 at 32 nM (double that predicted to specify digit 4). Simulating this model for 20 hr produced a limb with five digits with the pattern 2, 2, 3, 4, 4, with the four anterior digits arising from cells adjacent to the polarizing region instead of just the three (Fig. 5, Supp. Movie S6). The concentra-

tion of Shh predicted to specify a digit 5 was not breached in the allotted time, so that only a digit 4 developed from the polarizing region. Furthermore, the diffusion range of Shh signalling that would be required to specify the most-anterior digit in this model would be 660  $\mu\text{m}$ .

In order to see if we could simulate specification of the digit identities of the mouse limb more accurately, we took account of previous analyses suggesting that the five digits are specified in about 8 hr by a pulse of Shh, perhaps by a gradient (Zhu et al., 2008). According to our simulations for the chick wing and leg (see above), 8 hr is far too little time for a gradient of Shh to surpass the thresholds of five digits with identities being promoted in an anterior to posterior

sequence. Although there is no evidence of this specification phase, Zhu et al. (2008) suggested that digits then form in the order 1, 4, 2, 5, 3 according to the duration of Shh signalling required for subsequent survival of specified cells. This matches the digit patterns they obtained when Shh was removed at progressively later time-points: 1, 4, 1, 2, 4 and 1, 2, 4, 5 and finally 1, 2, 3, 4, 5. We have suggested that because of the unclear digit identities in the mouse limb these data might reflect the promotion of digit specification over time (Towers et al., 2011; see also Tabin and McMahon, 2008), although there is no direct evidence that promotion occurs in the mouse limb. Thus the digit patterns obtained upon Shh deletion could instead be: 1, 2 (not 1, 4), 1, 2, 3 (not 1, 2, 4), 1, 2, 3, 5 (not 1, 2, 4, 5), and finally 1, 2, 3, 4, 5, with the four anterior digits being specified in a similar fashion to the chick leg digits (Fig. 4), while digit 5 is specified independently of graded signalling, by a transient pulse of Shh signalling (Ahn and Joyner, 2004) and hence is the fourth digit of the pattern to be specified. To simulate this required us to impose an external conditional such that the polarizing region branches into two digit domains at a time when it is 145  $\mu\text{m}$  (70–75  $\mu\text{m}$  for each digit) in diameter when only three digit domains have been specified in the bud (Fig. 6, Supp. Movie S7). It can be seen that the periodic spacing of digit fields is altered across the limb bud such that digits derived from the polarizing region are spaced closer together than those specified by graded paracrine Shh signalling (Fig. 6, Supp. Movie S7). In addition, this simulation accurately replicates the transient digit patterns predicted when the chick leg promotion model is applied to the mouse limb (Fig. 6, Supp. Movie S7) (Towers et al., 2011). Thus it can be seen that, according to the simulation, the patterns, 1, 2, then 1, 2, 3 and 1, 2, 3, 5 are obtained if Shh signalling is curtailed at different times and digit 4 is the last to be specified (Fig. 6, Supp. Movie S7).

## DISCUSSION

We have shown that a mathematical model incorporating the core

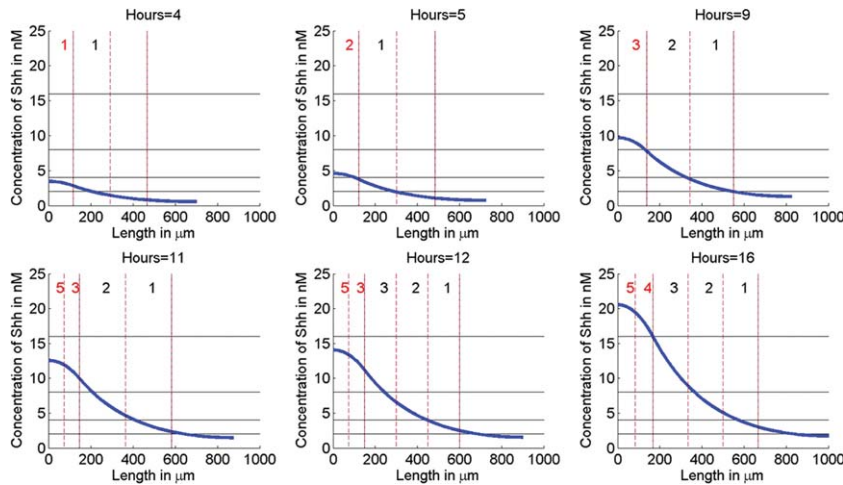


**Fig. 6.** (Supp. Movie S7). Specification of the mouse digit pattern by graded/transient Shh signalling. Solution of equation (1), with boundary conditions given by equation (2), on a uniformly linearly growing domain. Parameters are  $D = 24 \mu\text{m}^2/\text{s}$ ,  $\gamma = 1/60^2/\text{s}$ ,  $\alpha = 0.014/57600^2/\text{s}$  and  $r = 0.5/(43200)/\text{s}$ . The polarizing region branches into two digit domains at 11 hr (shown in red); the posterior one is instantly specified as digit 5 by transient Shh signalling. The rest of the digit pattern is specified by graded Shh signalling as the chick leg pattern (Fig. 4).

parameters of a classical-type Shh signalling gradient established by localised production, diffusion, and linear decay can simulate the temporal specification of the identities of the three chick wing digits. Digit number is specified by the size of the digit-forming field that is at least, in part, determined by Shh-dependent growth (Towers et al., 2008), but not by Shh gradient thresholds as predicted in earlier models (Wolpert and Hornbruch, 1981). It is of interest that the model still works without having to factor in cellular responses to Shh such as *Ptch1* accumulation, which acts to sequester Shh and dampen signalling. Moreover, the expression patterns of other cell surface co-receptors of Shh, including *Boc*, *Cdo*, and *Gas1* (Allen et al., 2011), means that they are unlikely to interfere with free Shh diffusion over the digit-forming field, but could instead have roles in modifying boundary conditions. Thus, for example, *Ptch1* is highly expressed in the polarizing region and could act to sequester and buffer Shh levels, and *Gas1* is expressed in the anterior part of the limb and could limit diffusion of Shh out of the digit-forming field. Furthermore, it is probable that *Ptch1* accumulation is proportional to the amount of Shh in the system since a 3-fold difference in Shh concentra-

tion (5–16 mg/ml soaking solution for beads) can give the same outcome in terms of digit pattern (Yang et al., 1997). In order to successfully model the chick leg digit pattern with four digits, none of the core parameters has to be altered, other than allowing a digit to arise from the Shh-producing cells of the polarizing region. This effectively increases the number of digits that Shh can specify without the need of increasing diffusion distance, the extent of which could otherwise be a constraint. Thus, our model suggests that three could be the maximum number of digits specified by paracrine Shh signalling in vertebrate limbs.

To simulate the mouse limb digit pattern, we had to alter the classical view of morphogen read-out and impose a condition such that the time of exposure to, and not concentration of, Shh is the key parameter in specifying digit 5 (Ahn et al., 2004). This is because the core parameters of the chick limb model could only specify four digits. In our simulation of the mouse limb, we noted that digits derived from the polarizing region were spaced closer together than those specified by graded Shh signalling. We estimate that the minimum digit domain forming in response to graded paracrine signalling is  $125 \mu\text{m}$  and to autocrine signalling is 70–75

$\mu\text{m}$ . One possibility explaining this roughly twofold difference is that a Turing-type reaction-diffusion system only interacts with positional values specified much earlier by paracrine Shh signalling to space cartilage condensations. The fact that the chick wing digit-forming field still forms three digits when it is reduced by half could mean that the periodicity of the Turing-type mechanism scales equivalently. Further reduction in growth of the digit-forming field results in loss of digits showing this scaling process has a limit that reveals the minimum digit domain size. Changes in the periodicity of digits in mouse mutants can be simulated by Turing-type models (Miura et al., 2006; Sheth et al., 2012). In the case of autocrine Shh signalling, a reaction-diffusion system might not be involved since growth directly leads to the formation of digits. Thus, minimum digit domain width would be determined by a threshold number of specified cells rather than limits to the periodicity of a reaction-diffusion system.

Domain growth is an integral feature of our models, being required for a concentration gradient of paracrine Shh signalling to specify positional values for each of the three anterior digits in vertebrate limbs. The chick wing simulation predicts that anterior digit identities are lost under the most restrictive growth conditions and this has been observed experimentally (Towers et al., 2008). In addition, growth of the polarizing region leads to an increase in production of Shh over time and can also eventually lead to sufficient cells to form a digit. A buffering system has been described involving cell death, which controls the number of cells expressing *Shh* in the chick wing and it is possible that this prevents concentration levels increasing further once specification is complete (Sanz-Ezquerro and Tickle, 2000). It is possible that cell death ensures that the polarizing region does not normally give rise to additional posterior digits in the chick wing and leg (Towers et al., 2011).

The models for specification of limb digits may represent general patterning principles and be relevant, for example, to specification of cell types along the dorso-ventral axis of the



neural tube. As in the wing bud, the concentration of Shh increases over time in the floor plate/notochord and there is substantial growth along the dorso-ventral axis of the neural tube (Chamberlain et al., 2008). These factors have not been taken into account in current models and instead the focus has been on changes in the sensitivity of the cellular response to Shh (Dessaud et al., 2008; Balaskas et al., 2012). In contrast, the specification of wing digits appears to involve a ratchet-type promotion mechanism (Tickle, 2006). Interestingly, however, there is evidence that graded signalling does not specify the fate of *Shh*-expressing cells of the floor plate (Ribes et al., 2010) analogous with digit 5 progenitors in the mouse limb (Ahn and Joyner, 2004). Therefore, in neural cell specification and mouse digit specification, a classical morphogen gradient model may not be sufficient to specify all cell/digit identities.

There is also a remarkable parallel between the two posterior digits of the mouse limb and the two posterior veins of insect wings, which arise from the *Hedgehog*-expressing cells of the posterior wing compartment and whose specification is independent of graded Hedgehog signalling (Blair, 2007). Taking this analogy further, it is possible that the polarizing region of the vertebrate limb constitutes a posterior compartment. Thus, in the vertebrate limb, as in the fly wing, an intersection of compartment boundaries at the tip could control the development of the signalling region (the apical ectodermal ridge in the vertebrate limb) responsible for outgrowth (Meinhardt, 1983).

## EXPERIMENTAL PROCEDURES

### Size of the Digit-Forming Field

Fate maps show that the initial size of the field in the chick wing bud is 300  $\mu\text{m}$  (Towers et al., 2008). This is consistent with experiments showing that an anteriorly grafted polarizing region can signal through 200  $\mu\text{m}$  of leg tissue placed between it and the host chick wing bud and

specify an additional host digit 2 (Honig, 1981).

### Time Taken for Digit Specification

Experiments in which Shh signalling was inhibited by cyclopamine show that it takes 12 hr to specify the three digits in the wing (Scherz et al., 2007; Towers et al., 2008), although in mouse and chick limbs, *Shh* transcripts are detectable for around 60 hr. This extended expression is due to Shh being required to maintain the apical ectodermal ridge and final digit morphology, i.e., the phalanx can be lost in the most-posterior digit of the chick wing and mouse limb when *Shh* expression is curtailed (Scherz et al., 2004). The 12-hr specification period in normal development contrasts with the 24 hr required to specify a complete duplicate digit pattern by polarizing region grafts (Smith, 1980), retinoic acid-soaked beads (Tickle et al., 1985) (which induce *Shh* expression), or Shh-soaked beads (Yang et al., 1997) placed at the anterior margin of the wing bud (see Tickle, 2006). This discrepancy can be explained by the likelihood that induction of a duplicate digit pattern involves a priming phase during which anterior wing bud cells are made competent to form digits (Eichele et al., 1985).

### Growth Rate of the Digit-Forming Field and Digit Number Specification

Digits are specified over 12 hr (Towers et al., 2011) and final digit number is proportional to the size of the digit-forming field that is controlled by Shh. Digits are equally spaced across this field and the following measurements are taken from Towers et al. (2008). During normal development, the digit-forming field grows uniformly and linearly and its length increases by 50% from 300 to 450  $\mu\text{m}$  (150  $\mu\text{m}$  for each digit). Normal pattern still forms when digit field expansion is halved from 300 to 375  $\mu\text{m}$  (125  $\mu\text{m}$  for each digit). This is the minimum size for a digit domain and is consistent with the findings that two digits form in a 300- $\mu\text{m}$

domain and one digit in a 200- $\mu\text{m}$  domain.

### Shh Thresholds That Specify Digit Identities

Experiments in which defined numbers of polarizing region cells (Tickle et al., 1981) or beads soaked in Shh protein (Yang et al., 1997) were grafted to the anterior margin of chick wing buds indicate that a doubling in cell number or Shh concentration (in solution in which beads are soaked) is required to specify a digit 2 versus a digit 3 and a digit 3 versus a digit 4. Shh (4 nM) induces floor plate markers in neural tube explants (Ribes et al., 2010) and grafts of floor plate to the anterior margin of chick wing buds induce digit 3 identity (Wagner et al., 1990) suggesting that 2 nM Shh would specify a digit 2, 4 nM would specify a digit 3, and 8 nM would specify a digit 4. Digits are promoted through progressively more-posterior positional values every 4 hr, i.e., cells closest to the polarizing region transit through digit 1 fate at 4 hr, digit 2 fate at 8 hr, and then finally give rise to a digit 3 at 12 hr (Towers et al., 2011). In our model, a digit identity is specified when a digit domain is 125  $\mu\text{m}$  or more (minimum digit domain size) and the average Shh threshold within this domain breaches a given threshold concentration. Thus to produce an anterior-to-posterior 1, 2, 3 pattern, the average concentration of Shh in the most anterior digit domain needs to be greater than 2 nM, the average concentration of Shh in the middle digit domain needs to be greater than 4 nM, and the average concentration of Shh in the most-posterior domain needs to be greater than 8 nM.

### Degradation and Diffusion Rates of Shh

The diffusion rates of Shh in chick wing bud tissue used in our equations are estimated and are the same order of magnitude as those used in previous studies. The degradation and diffusion rates of Shh protein are taken to be  $\gamma = 1/60^2$  /s and  $D = 24 \mu\text{m}^2/\text{s}$ ,

respectively (Dillon et al., 2003; Saha and Schaffer, 2006).

## ACKNOWLEDGMENTS

M.T. and C.T. thank the MRC; C.T. was a Royal Society Professor and subsequently supported by an Emeritus Fellowship from The Leverhulme Trust.

## REFERENCES

- Ahn S, Joyner AL. 2004. Dynamic changes in the response of cells to positive hedgehog signaling during mouse limb patterning. *Cell* 118:505–516.
- Allen BL, Song JY, Izzi L, Althaus IW, Kang JS, Charron F, Krauss RS, McMahon AP. 2011. Overlapping roles and collective requirement for the coreceptors GAS1, CDO, and BOC in SHH pathway function. *Dev Cell* 14:775–787.
- Balaskas N, Ribeiro A, Panovska J, Dessaud E, Sasai N, Page KM, Briscoe J, Ribes V. 2012. Gene regulatory logic for reading the Sonic Hedgehog signaling gradient in the vertebrate neural tube. *Cell* 148:273–284.
- Benson DL, Maini PK, Sherratt JA. 1993. Diffusion driven instability in an inhomogeneous domain. *Bull Math Biol* 55:365–384.
- Blair SS. 2007. Wing vein patterning in *Drosophila* and the analysis of intercellular signaling. *Annu Rev Cell Dev Biol* 23:293–19.
- Chamberlain CE, Jeong J, Guo C, Allen BL, McMahon AP. 2008. Notochord-derived Shh concentrates in close association with the apically positioned basal body in neural target cells and forms a dynamic gradient during neural patterning. *Development* 135:1097–1106.
- Chiang C, Litingtung Y, Lee E, Young KE, Corden JL, Westphal H, Beachy PA. 1996. Cyclopia and defective axial patterning in mice lacking sonic hedgehog function. *Science* 383:407–413.
- Cooke J, Summerbell D. 1980. Cell cycle and experimental pattern duplication in the chick wing during embryonic development. *Nature* 287:697–701.
- Crampin EJ, Gaffney EA, Maini PK. 1999. Reaction and diffusion on growing domains: scenarios for robust pattern formation. *Bull Math Biol* 61:1093–1120.
- Dessaud E, McMahon AP, Briscoe J. 2008. Pattern formation in the vertebrate neural tube: a sonic hedgehog morphogen-regulated transcriptional network. *Development* 135:2489–2503.
- Dillon R, Gadgil C, Othmer HG. 2003. Short- and long-range effects of Sonic hedgehog in limb development. *Proc Natl Acad Sci USA* 100:10152–10157.
- Drossopoulou G, Lewis KE, Sanz-Ezquerro JJ, Nikbakht N, McMahon AP, Hofmann C, Tickle C. 2000. A model for anteroposterior patterning of the vertebrate limb based on sequential long- and short-range Shh signalling and Bmp signalling. *Development* 127:1337–1348.
- Eichele G, Tickle C, Alberts BM. 1985. Studies on the mechanism of retinoid-induced pattern duplications in the early chick limb bud: temporal and spatial aspects. *J Cell Biol* 101:1913–1920.
- French V, Bryant PJ, Bryant SV. 1976. Pattern regulation in epimorphic fields. *Science* 193:969–981.
- Glimm T, Headon D, Kiskowski MA. 2012a. Computational and mathematical models of chondrogenesis in vertebrate limbs. *Birth Defects Res C Embryo Today* 96:176–192.
- Glimm T, Zhang J, Shen YQ, Newman SA. 2012b. Reaction-diffusion systems and external morphogen gradients: the two-dimensional case, with an application to skeletal pattern formation. *Bull Math Biol* 74:666–687.
- Hentschel HG, Glimm T, Glazier JA, Newman SA. 2004. Dynamical mechanisms for skeletal pattern formation in the vertebrate limb. *Proc Biol Sci* 271:1713–1722.
- Honig LS. 1981. Positional signal transmission in the developing chick limb. *Nature* 291:72–73.
- Izaguirre JA. 2004. Chaturvedi R, Huang C, Cickovski T, Coffland J, Thomas G, Forgacs G, Alber M, Hentschel G, Newman SA, Glazier JA. *CompuCell*, a multi-model framework for simulation of morphogenesis. *Bioinformatics* 20:1129–1137.
- Marigo V, Scott MP, Johnson RL, Goodrich LV, Tabin CJ. 1996. Conservation in hedgehog signaling: induction of a chicken patched homolog by Sonic hedgehog in the developing limb. *Development* 122:1225–1233.
- Meinhardt H. 1983. A boundary model for pattern formation in vertebrate limbs. *J Embryol Exp Morphol* 76:115–137.
- Miura T, Shiota K, Morriss-Kay G, Maini PK. 2006. Mixed-mode pattern in Doublefoot mutant mouse limb: Turing reaction-diffusion model on a growing domain during limb development. *J Theor Biol* 240:562–573.
- Newman SA, Frisch HL. 1979. Dynamics of skeletal pattern formation in developing chick limb. *Science* 205:662–668.
- Newman SA, Christley S, Glimm T, Hentschel HG, Kazmierczak B, Zhang YT, Zhu J, Alber M. 2008. Multiscale models for vertebrate limb development. *Curr Top Dev Biol* 81:311–340.
- Ribes V, Balaskas N, Sasai N, Cruz C, Dessaud E, Cayuso J, Tozer S, Yang LL, Novitch B, Marti E, Briscoe J. 2010. Distinct Sonic Hedgehog signaling dynamics specify floor plate and ventral neuronal progenitors in the vertebrate neural tube. *Genes Dev* 24:1186–1200.
- Riddle RD, Johnson RL, Laufer E, Tabin C. 1993. Sonic hedgehog mediates the polarizing activity of the ZPA. *Cell* 75:1401–1416.
- Ros MA, Dahn RD, Fernandez-Teran M, Rashka K, Caruccio NC, Hasso SM, Bitgood JJ, Lancman JJ, Fallon JF. 2003. The chick oligozeugodactyly (ozd) mutant lacks sonic hedgehog function in the limb. *Development* 130:527–537.
- Saha K, Schaffer DV. 2006. Signal dynamics in Sonic hedgehog tissue patterning. *Development* 133:889–900.
- Sanz-Ezquerro JJ, Tickle C. 2000. Autoregulation of Shh expression and Shh induction of cell death suggest a mechanism for modulating polarising activity during chick limb development. *Development* 127:4811–4823.
- Saunders JW, Gasseling MT. 1968. Ectodermal-mesenchymal interactions in the origin of limb symmetry. In: Fleischmeyer R, Billingham RE, editors. *Mesenchymal-epithelial interactions*. Baltimore: Williams and Wilkins, p 78–97.
- Scherz PJ, McGlinn E, Nissim S, Tabin CJ. 2007. Extended exposure to Sonic hedgehog is required for patterning the posterior digits of the vertebrate limb. *Dev Biol* 308:343–354.
- Sheth R, Marcon L, Bastida MF, Junco M, Quintana L, Dahn R, Kmita M, Sharpe J, Ros MA. 2012. Hox genes regulate digit patterning by controlling the wavelength of a Turing-type mechanism. *Science* 338:1476–1480.
- Smith JC. 1980. The time required for positional signalling in the chick wing bud. *J Embryol Exp Morphol* 60:321–328.
- Smith JC, Tickle C, Wolpert L. 1978. Attenuation of positional signalling in the chick limb by high doses of gamma-radiation. *Nature* 272:612–613.
- Summerbell D, Tickle C. 1977. Pattern formation along the anterior-posterior axis of the chick limb bud. In: Ede DA, Hinchliffe JR, Balls M, editors. *Vertebrate limb and somite morphogenesis*. Cambridge: Cambridge University Press. p 41–53.
- Tabin CJ, McMahon AP. 2008. Grasping limb patterning. *Science* 321:350–352.
- Tamura K, Nomura N, Seki R, Yonei-Tamura S, Yokoyama H. 2011. Embryological evidence identifies wing digits in birds as digits 1, 2, and 3. *Science* 331:753–757.
- Tickle C. 1981. The number of polarizing region cells required to specify additional digits in the developing chick wing. *Nature* 289:295–298.
- Tickle C. 1995. Vertebrate limb development. *Curr Opin Genet Dev* 5:478–484.
- Tickle C. 2006. Making digit patterns in the vertebrate limb. *Nature Rev* 7:45–53.
- Tickle C, Summerbell D, Wolpert L. 1975. Positional signalling and specification of digits in chick limb morphogenesis. *Nature* 254:199–202.
- Tickle C, Lee J, Eichele G. 1985. A quantitative analysis of the effect of all-trans-retinoic acid on the pattern of chick wing development. *Dev Biol* 109:82–95.
- Towers M, Tickle C. 2009. Growing models of vertebrate limb development. *Development* 136:179–190.
- Towers M, Manhood R, Yin Y, Tickle C. 2008. Integration of growth and



- specification in chick wing digit-patterning. *Nature* 452:882–886.
- Towers M, Signolet J, Sherman A, Sang H, Tickle C. 2011. Insights into bird wing evolution and digit specification from polarizing region fate maps. *Nat Commun* 2:426.
- Vargesson N, Clarke JD, Vincent K, Coles C, Wolpert L, Tickle C. 1997. Cell fate in the chick limb bud and relationship to gene expression. *Development* 124:1909–1918.
- Wagner M, Thaller C, Jessell T, Eichele G. 1990. Polarizing activity and retinoid synthesis in the floor plate of the neural tube. *Nature* 345:819–822.
- Wilby OK, Ede DA. 1975. A model generating the pattern of cartilage skeletal elements in the embryonic chick limb. *J Theor Biol* 52:199–217.
- Wolpert L. 1969. Positional information and the spatial pattern of cellular formation. *J Theor Biol* 25:1–47.
- Wolpert L, Hornbruch A. 1981. Positional signalling along the anteroposterior axis of the chick wing. The effect of multiple polarizing region grafts. *J Embryol Exp Morphol* 63:145–159.
- Yang Y, Drossopoulou G, Chuang PT, Duprez D, Marti E, Bumcrot D, Vargesson N, Clarke J, Niswander L, McMahon A, Tickle C. 1997. Relationship between dose, distance and time in Sonic Hedgehog-mediated regulation of anteroposterior polarity in the chick limb. *Development* 124:4393–4404.
- Zeng X, Goetz JA, Suber LM, Scott WJ Jr., Schreiner CM, Robbins DJ. 2001. A freely diffusible form of Sonic hedgehog mediates long-range signalling. *Nature* 411:716–720.
- Zhu J, Nakamura E, Nguyen MT, Bao X, Akiyama H, Mackem S. 2008. Uncoupling Sonic hedgehog control of pattern and expansion of the developing limb bud. *Dev Cell* 14:624–632.